Route Planning of Fixed-Wing Unmanned Aerial Vehicles for Maritime Communication Coverage

Jingwei Li
Dept. of Electronic Engineering
Tsinghua University
Beijing, China
lijingwe20@mails.tsinghua.edu.cn

Xiaofeng Zhong
Dept. of Electronic Engineering
Tsinghua University
Beijing, China
zhongxf@tsinghua.edu.cn

Shidong Zhou
Dept. of Electronic Engineering
Tsinghua University
Beijing, China
zhousd@tsinghua.edu.cn

Xuemeng Gong
Dept. of Electronic Engineering
Beijing Jiaotong University
Beijing, China
22125024@bjtu.edu.cn

Jie Wei
Dept. of Electronic Engineering
Beijing Jiaotong University
Beijing, China
jwei@bjtu.edu.cn

***Abstract*— The problem of route planning is important for setting up communication base station based on unmanned aerial vehicle (UAV). This paper proposes a route planning algorithm by creating control points and route patterns in the resource-limited scenario of maritime communication. The algorithm could realize the route planning under coupling constraints of the UAV communication base stations' total number, transmission distance, flight speed and turning radius. The simulation result shows a significant improvement than existing methods. The minimum on-line rate of the users obtained by the algorithm proposed in this paper is up to 33% higher than the former algorithm, and up to 54% higher than distribute the UAVs evenly. The increase of the average on-line rate also gets a slightly improvement up to 16% and 27% respectively.**

***Keywords*— maritime communication, unmanned aerial vehicle, route planning**

I. INTRODUCTION

It is of great practical significance to study and build a highly reliable and easily organized maritime communication network specially. There are many differences between maritime communication and land communication. For example, maritime communication lacks shore-based facilities, and most of its users are temporary and mobile. The use of unmanned aerial vehicle (UAV) to carry communication base stations can better meet the above needs. Because UAV can fly above the sea with the advantage of flexible deployment, comprehensive functions, etc. [1] [2].

There have been many researches on route planning algorithms of point-to-point mission and area traversal mission of UAV [3] [4]. These studies can be used for single-point and short-term tasks, but not for long-term large area networking. UAV needs to accompany the users to fly back and forth in an area during the long-term tasks, thus the route planning should mainly consider its communication coverage to ensure the realization of networking. At present, the research object for this problem is mainly rotor-wing UAV. There are many differences between rotor-wing UAV and fixed-wing UAV with higher flight altitude, greater payload and stronger range capability. The rotor-wing UAV only needs to consider the maximum flight speed, then connect the calculated optimal position at each moment to form a continuous route, while the fixed-wing UAV will be restricted by the minimum flight speed, minimum turning radius, rolling effect and other factors. Reference [6] proposed a route planning method based on K-means clustering. Reference [7] proposed another method based on the weighted centroid of the users. Neither of them is suitable for fixed-wing UAV, especially under the condition of limited resources, because they did not take into account the constraint of the flight speed and the transmission distance of the UAV communication base station.

Therefore, a new route planning algorithm is proposed in this paper. This paper focuses on fixed-wing UAV under the condition of limited resources. Through the steps of grouping the users, setting and filtering the control points, plotting and smoothing the route patterns, the route plan under the coupling restriction of the flight speed, the turning radius and turning slope, the transmission distance and the total number of the UAV communication base stations is realized. Simulation results show that the users' average on-line rate and minimum on-line rate obtained by the proposed algorithm are increased by up to 16% and 33% respectively compared with the existing algorithms, and by up to 27% and 54% respectively compared with the method of evenly distributing the UAV communication base stations.

II. SYSTEM MODEL

A. Users' Model

Considering the circular target sea area with radius R, there are several communication users in static or moving state on the sea surface. Set the total number of the users as J, and the initial positions of all users are randomly distributed in the target sea area. The users make random motion at a speed within a certain range in the time from 0 to T. The jth user's position at time t is marked as $W_j(j,t)$, expressed in $\left[x_j(j,t), y_j(j,t)\right]$, its speed is marked as $v_j(j,t)$, and its direction is marked as $\alpha_j(j,t)$, $j=1,2,...,J$.

Fig. 1 shows a group of users' track data randomly generated under the conditions of R=8km, J=20, T=120min, and $v_j(j,t)\in(0.5\text{km/min}, 0.7\text{km/min})$. Each curve represents an user's continuous track.

Fig. 1. The example of the users' track.

B. UAVs' Model

Similar to the users' variables, the total number of the UAVs is marked as I, the ith UAV's position at time t is marked as $W_I(i,t)$, expressed in $\left[x_I(i,t), y_I(i,t)\right]$, its speed is marked as $v_I(i,t)$, and its direction is marked as $\alpha_I(i,t)$, $i=1,2,...,I$. The study is based on large fixed-wing UAVs. There are constraints such as maximum flight speed $v_{I\max}$, minimum flight speed $v_{I\min}$ and minimum turning radius $r_{I\min}$ during the flight of the UAVs, and there will be a turning slope with an angle of θ_I during the turning process. The $\cot(\theta_I)$ is proportional to the turning radius r_I [8].

C. Channels' Model

The research shows that the maritime wireless communication has a relatively complex channel model under the coupling effect of free space loss, reflection loss, atmospheric absorption loss, etc., the external factors such as ground equivalent reflection coefficient, water vapor density, etc. will affect the signal transmission effect [9] [10]. It is assumed that there is no significant difference in the ground equivalent reflection coefficient and water vapor density for the same sea area at the same time. When the communication frequency and antenna height are fixed, it can be approximated that the path loss of sea-air communication is mainly related to the distance d_{IJ} between the user and the communication base station.

Suppose that the antennas carried by the UAVs and the users are both omnidirectional antennas. The antennas carried by the UAVs are located in the belly of the UAV, the transmission directions towards the fuselage will be greatly attenuated due to the obstruction, and the other transmission directions will have a same maximum transmission distance marked as D_Z. The coverage of an UAV communication base station can be regarded as a hemisphere with the UAV as the center and D_Z as the radius. When an UAV is flying horizontally, its hemisphere will intersect with the sea level to form a circular section. This circular section is the effective range that the users on the water surface could communicate with the UAV, it is called the coverage at sea level, as shown in Fig. 2.

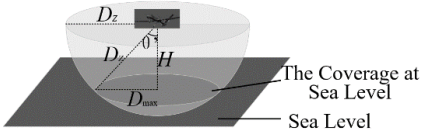

Fig. 2. The coverage when the UAV is flying horizontally.

If the flight altitude of the UAV is H, the radius $D_{\max}$ of the coverage at sea level can be expressed as:

$$D_{\max} = \sqrt{D_Z^{\,2} - H^2} \tag{1}$$

The angle θ' between the line from the UAV communication base station to the farthest position of the coverage at sea level and the normal of sea level can be expressed as:

$$\theta' = \cos^{-1}\left(H/D\right) \tag{2}$$

The UAV will roll inward during the turning process due to the centripetal force, that is, there will be a turning slope θ_I. When $\theta_I \le (\pi/2) - \theta'$, the coverage at sea level is still a circle with a radius of $D_{\max}$; When $\theta_I > (\pi/2) - \theta'$, the coverage at sea level will be reduced to an incomplete circle, as shown in Fig. 3 and Fig. 4:

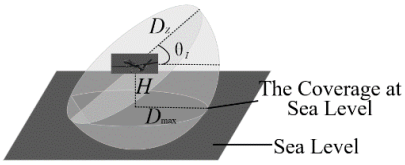

Fig. 3. The coverage when the UAV is turning.

The polar coordinate expression of the coverage at sea level based on (ρ,φ) is:

$$\rho = \begin{cases} \left(H \bullet \cot\theta_I\right)/\cos\varphi, & \pi-\omega<\varphi<\pi+\omega \\ D_{\max}, & \varphi \ge \pi+\omega \cup \varphi \le \pi-\omega \end{cases} \tag{3}$$

$$\omega = \cos^{-1}\left[\left(H \bullet \cot\theta_I\right)/D_{\max}\right] \tag{4}$$

It can be seen from (3) and (4) that whether the UAV's rolling inward will affect the coverage at sea level mainly depends on $H \bullet \cot\theta$. When $H \bullet \cot\theta \le D_{\max}$, the coverage at sea level will not be affected.

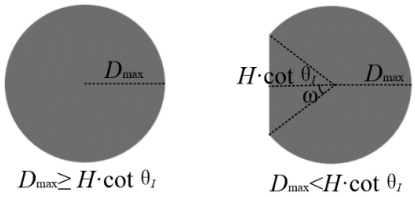

Fig. 4. Top view of the coverage at sea level when the UAV is turning.

III. ROUTE PLANNING ALGORITHM

This algorithm is mainly aimed at improving the average on-line rate P_{ave} and the minimum on-line rate $P_{\min}$ of how the users connecting with the UAV communication base stations. If the total number of timeslots is N, there are $N_J(j)$ timeslots in which the jth user has successfully established a communication link with any UAV communication base station in all N timeslots, there will be:

$$P_{\text{ave}} = \left[\sum_{j=1}^{J} N_J(j)\right] \Big/ (N \bullet J) \tag{5}$$

$$P_{\min} = \min_{j=1,2,...,J}\left[N_J(j)/N\right] \tag{6}$$

This algorithm is specially designed for getting a result with a higher P_{ave}, and the $P_{\min}$ is as high as possible at the same time. The process is as shown in Fig. 5:

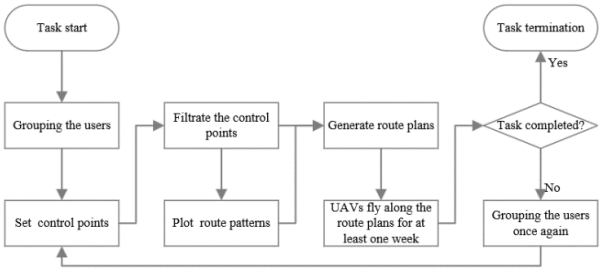

Fig. 5. The flow chart of the route planning algorithm.

A. Grouping the users

The users should be grouped to delimit the task scope of each UAV. Because the overlap of UAVs' coverage should be avoided as much as possible in order to maximize the coverage effect of multiple UAV communication base stations.

K-means clustering method can divide several users into a specified number of groups through iterative solution, and the sum of the squares of the error of each user's distance from the group centroid is locally minimum [11]. The algorithm in this paper uses K-means clustering to group the users at time *t*, and the number of the clustering groups is equal to the number of UAV communication base stations *I*. Taking the users' data shown in Fig. 1 as an example, its grouping result at time t = 0 is shown in Fig. 6. The total number of the grouping operations is recorded as *M*.

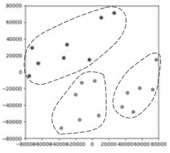

Fig. 6. The grouping result at time $t = 0$.

B. Planning in Different Groups

The route planning of the UAVs will be carried out independently in each grouping area. The main steps are as follows.

1) Set Control Points

Since the users are also in motion during the flight of the UAVs, a control coefficient $\sigma \in (0,1]$ is set, and $\sigma \bullet D_{\max}$ is used as the control distance for setting control points.

Assuming that the number of the users in the *i*th group of the *m*th grouping operation is $J_0(m,i)$, the position of the *j*th user in the group is marked as $W_{J0}(m,i,j)$, expressed in $\left[x_{J0}(m,i,j), y_{J0}(m,i,j)\right]$. The cluster center of the group is marked as $Z_0(m,i)$, expressed in $\left[x_{Z0}(m,i), y_{Z0}(m,i)\right]$. The Euclidean distance between $W_{J0}(m,i,j)$ and $Z_0(m,i)$ is marked as $d_0(m,i,j)$. If $d_0(m,i,j) > \sigma \bullet D_{\max}$, the position after $W_{J0}(m,i,j)$ shifts $\sigma \bullet D_{\max}$ distance to $Z_0(m,i)$ direction will be taken as a control point; If $d_0(m,i,j) \le \sigma \bullet D_{\max}$, $Z_0(m,i)$ will be taken as a control point; If multiple control points coincide, only one of them will be retained.

The total number of the control points in the *i*th group is marked as $J_1(m,i)$, their geometric centroid is marked as $Z_1(m,i)$, expressed in $\left[x_{Z1}(m,i), y_{Z1}(m,i)\right]$. The position of the *j*th control point in the *i*th group is marked as $W_{J1}(m,i,j)$, expressed in $\left[x_{J1}(m,i,j), y_{J1}(m,i,j)\right]$. The orders of these control points are arranged counterclockwise in the direction from $W_{J1}(m,i,j)$ to $Z_1(m,i)$. If $W_{J1}(m,i,j)$ is obtained by the translation of $W_{J0}(m,i,k)$, there will be:

$$x_{J1}(m,i,j) = d_1 \bullet \left[x_{J0}(m,i,k) - x_{Z0}(m,i)\right] + x_{Z0}(m,i) \quad (7)$$

$$y_{J1}(m,i,j) = d_1 \bullet \left[y_{J0}(m,i,k) - y_{Z0}(m,i)\right] + y_{Z0}(m,i) \quad (8)$$

$$d_1 = 1 - \frac{\sigma \bullet D_{\max}}{d_0(m,i,k)} \quad (9)$$

The comparison between the positions of the users and the control points is shown in Fig. 7.

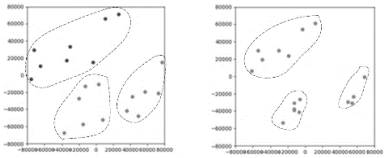

Fig. 7. The comparison between the users (the left one) and the control points (the right one).

2) Filtrate the Control Points and Plot Route Patterns

The control points will need to be filtered if $J_1(m,i)$ is greater than 2. The selected control points will be connected to form a polygon with the shortest perimeter, all control points will be enclosed by the polygon. Each inner corner of the polygon should be less than 180° in order to ensure the shortest perimeter.

Define the operation symbol $\oplus$, for $j,k = 1,2,...,J$, when $j+k \le J$, there is $j \oplus k = j+k$; When $j+k > J$, there is $j \oplus k = j+k-J$.

Make a straight line through $W_{J1}(m,i,j)$ and $W_{J1}(m,i,j\oplus 2)$, and another straight line through $Z_1(m,i)$ and $W_{J1}(m,i,j\oplus 1)$. The intersection of these two lines are recorded as $Z_2(m,i,j)$. If $W_{J1}(m,i,j\oplus 1)$ and $Z_2(m,i,j)$ are coinciding, it means that $W_{J1}(m,i,j)$, $W_{J1}(m,i,j\oplus 1)$, and $W_{J1}(m,i,j\oplus 2)$ are on the same line; If $W_{J1}(m,i,j\oplus 1)$ locates between $Z_1(m,i)$ and $Z_2(m,i,j)$, it means that the inner corner of the polygon at $W_{J1}(m,i,j\oplus 1)$ is larger than 180°. In both cases, $W_{J1}(m,i,j\oplus 1)$ should be discarded. After filtering, the remaining control points will form a closed polygon, as shown in Fig.8, which is called the route pattern.

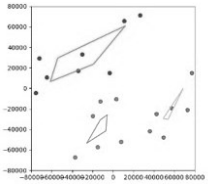

Fig. 8. The comparison between the users and the route pattern.

The total number of the remaining control points in the *i*th group is recorded as $J_2(m,i)$. The position of the *j*th remaining control point in the *i*th group is marked as $W_{J2}(m,i,j)$, expressed in $\left[x_{J2}(m,i,j), y_{J2}(m,i,j)\right]$. The linear equation from $W_{J2}(m,i,j)$ to $W_{J2}(m,i,j\oplus 1)$ is recorded as $y=a(m,i,j)\bullet x+b(m,i,j)$. The direction angle of $W_{J2}(m,i,j\oplus 1)$ relative to $W_{J2}(m,i,j)$ is recorded as $\alpha(m,i,j)$.

3) Generate the Route Plans

It is necessary to smooth the route pattern to form a realizable route plan because the fixed-wing UAV has a minimum turning radius constraint.

If $J_2(m,i)=1$, the *i*th UAV communication base station will move around $W_{J2}(m,i,1)$ in a circle. Its smooth route $\left[x_K(m,i), y_K(m,i), k\right]$ can be expressed as:

$$\begin{cases} k\in(0,2\pi] \\ x_K(m,i)=x_{j2}(m,i,1)+r_I\bullet\cos k \\ y_K(m,i)=y_{j2}(m,i,1)+r_I\bullet\sin k \end{cases} \tag{10}$$

If $J_2(m,i)>1$, first make control circles with each control point as the center and r_I as the radius, then connect each control circle with a common tangent according to the sequence of the control points to form a smooth and closed route. Fig. 9 shows the route planning results under three typical scenarios. There is one control point in Scenario (a), two control points in Scenario (b), and multiple control points in Scenario (c).

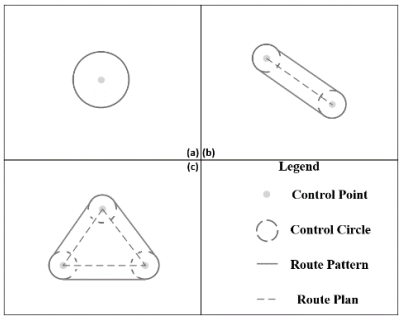

Fig. 9. The route planning results under three typical scenarios.

Except for Scenario (a), the route plan generated in the other two scenarios can be divided into $J_2(m,i)\times 2$ segments, in which $J_2(m,i)$ segments are straight lines that can be seen as the result of the route pattern $y=a(m,i,j)\bullet x+b(m,i,j)$ being translated outward equal to the distance of r_I; Another $J_2(m,i)$ segments are arcs with radius r_I, the total length of them equal to a whole circle with radius r_I. The expression of the smooth route $\left[x_K(m,i), y_K(m,i), k\right]$ can be expressed as:

$$G=J_2(m,i,j) \tag{11}$$

$$A(m,i,j)=\alpha(m,i,j)-0.5\times\pi \tag{12}$$

$$c(m,i,j)=-r_I/\cos\alpha(m,i,j) \tag{13}$$

$$b^*(m,i,j)=b(m,i,j)+c(m,i,j) \tag{14}$$

$$\begin{cases} k\in\left(A(m,i,G),\ A(m,i,G)+2\pi\right] \\ if\left[k\in\left(A(m,i,G),A(m,i,1)\right)\right]: \\ \quad\begin{cases} x_K(m,i)=x_{J2}(m,i,1)+r_I\bullet\cos k \\ y_K(m,i)=y_{J2}(m,i,1)+r_I\bullet\sin k \end{cases} \\ if\left[k=A(m,i,1)\right]: \\ \quad y_K(m,i)=a(m,i,1)\bullet x_K(m,i)+b^*(m,i,1) \\ if\left[k\in\left(A(m,i,1),A(m,i,2)\right)\right]: \\ \quad\begin{cases} x_K(m,i)=x_{J2}(m,i,2)+r_I\bullet\cos k \\ y_K(m,i)=y_{J2}(m,i,2)+r_I\bullet\sin k \end{cases} \\ if\left[k=A(m,i,2)\right]: \\ \quad y_K(m,i)=a(m,i,2)\bullet x_K(m,i)+b^*(m,i,2) \\ \cdots \\ if\left[k\in\left(A(m,i,G)-1,A(m,i,G)+2\pi\right)\right]: \\ \quad\begin{cases} x_K(m,i)=x_{J2}(m,i,G)+r_I\bullet\cos k \\ y_K(m,i)=y_{J2}(m,i,G)+r_I\bullet\sin k \end{cases} \\ if\left[k=A(m,i,G)+2\pi\right]: \\ \quad y_K(m,i)=a(m,i,G)\bullet x_K(m,i)+b^*(m,i,G) \end{cases} \tag{15}$$

C. Update the Route Plans

After the route planning is completed, the UAVs will fly in cycles according to the route plans until all the UAVs have completed at least one cycle. This moment is marked as T_m, which is related to the flight speed of the UAVs. The *m* represents the number of completed route planning. Then the $m+1$th planning should be carried out according to the users' location at moment T_m, the method is the same as the above.

After the completion of the new planning, the UAVs will access the nearest control circle in the new route plans with the double counterclockwise Dubins curve [12] from the position at moment T_m, then continue to fly along the new plans as shown in Fig.10.

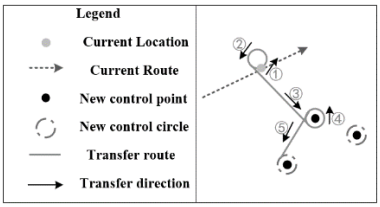

Fig. 10. Switch between different route plans.

Taking the users' data shown in Fig. 1 as an example, the continuous route plan formed by twice consecutive route planning is shown in Fig. 11.

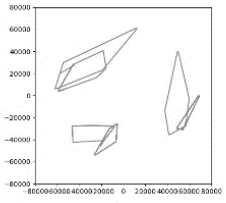

Fig. 11. The continuous route plan formed by twice consecutive route planning.

IV. Simulation Results

In order to verify the effectiveness of the proposed algorithm, the algorithm is implemented by Python compiler software, and multiple groups of users' track information are randomly generated. The algorithm proposed in this paper will be compared with the method based on K-means clustering in [6], the method based on the weighted centroid of the users in [7], and the method of evenly distributing the UAV communication base stations in the task area. Because the fixed-wing UAV cannot stay in a fixed position, the flight mode of the UAVs in the control groups is adjusted according to the fixed-wing UAV, they will circle around the fixed point instead of hovering there.

A. The Design of the Simulation

1) The background of the simulation

In combination with the actual situation, the simulations set the users' movement speed between 0.5 km and 0.7 km per minute, their course change shall not exceed 30 degrees in 1 minutes. The total number of the users is J=20.

The UAV communication base stations refer to the large fixed-wing UAV model, its flight altitude is $H = 6\text{km}$, cruise speed is $v_I(t) \in (2.5\text{km/min}, 3\text{km/min})$, and the minimum turning radius is $r_{I\min} = 0.5\text{km}$. The minimum turning radius has a turning slope $\theta_{I\max} = 20°$ when turning. The total number of the UAV communication base stations I, the radius of the coverage at sea level $D_{\max}$, and the turning radius r_I are the control variables.

The total duration of the task is 120 min, and the range of the task is a circular sea area with a radius of R=8km, the control coefficient $\sigma = 0.8$. Each group of simulations will randomly generate 10 groups of users' data and randomly select the starting point of the UAVs to conduct 100 independent repeated tests. The users' on-line status is calculated every 2 seconds during the flight of the UAVs.

2) The Control groups

Control group A: evenly distributing the UAV communication base stations in the task area. Select I fixed points in the task area evenly, and the UAVs will move around the fixed point in a circle with a radius of 5km, during which a turning slope $\theta_I = 2.1°$ will be generated. The turning slope will not affect the radius of the coverage at sea level. The schematic diagram of how the fixed points will be distributed is shown in Fig. 12:

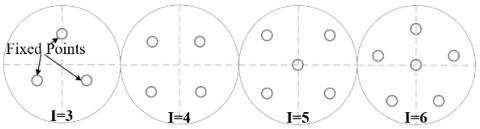

Fig. 12. Distribut the fixed points evenly in the task area.

Control group B: the method based on K-means clustering. According to the method proposed in [6], the users will be grouped every 10 minutes by using the K-means clustering algorithm. The UAVs move around the center of the group in a circle with a radius of 5km, during which a turning slope $\theta_I = 2.1°$ will be generated, same as the control group A.

Control group C: the method based on the weighted centroid of the users. According to the method proposed in [7], first use the K-means clustering to group the users into different groups at t=0, and then group all the users according to the location of the UAVs every 10 minutes. The UAVs move around the centroid of the group in a circle with a radius of 5km, during which a turning slope $\theta_I = 2.1°$ will be generated, same as the control group A.

B. The Result of the Simulation

1) Comparison between the proposed algorithm and the control groups

When $D_{\max} = 30\text{km}$, $r_I = 1\text{km}$, carry out control variable simulations on different I. The results are shown in Fig. 13 and Fig. 14.

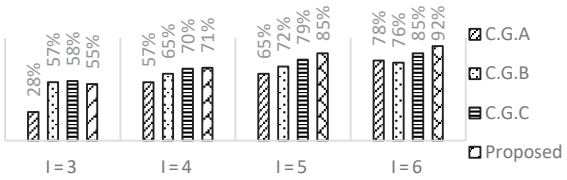

Fig. 13. The comparison of P_{ave} under different I

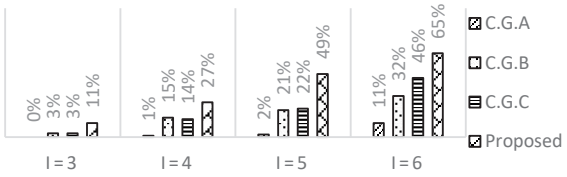

Fig. 14. The comparison of $P_{\min}$ under different I

When $I = 4$, $r_I = 1\text{km}$ carry out control variable simulations on different $D_{\max}$. The results are shown in Fig. 15 and Fig. 16. The dimension of $D_{\max}$ is km.

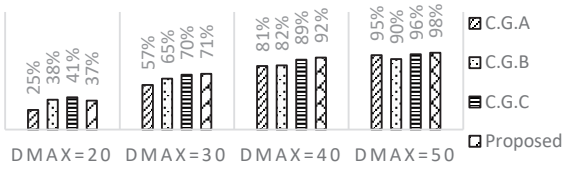

Fig. 15. The comparison of P_{ave} under different $D_{\max}$

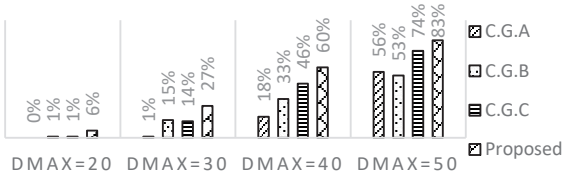

Fig. 16. The comparison of $P_{\min}$ under different $D_{\max}$

The simulations above proved that the algorithm proposed in this paper can achieve higher P_{ave} and higher P_{min} than the control group A and B. Although the P_{ave} of the proposed algorithm is similar to that of the control group C, it has achieved a relatively large improvement in P_{min}. Under the condition of limited resources, the algorithm proposed in this paper ensures better communication coverage.

2) Comparison of different parameters in the proposed algorithm

For the proposed algorithm, when $I=4$, carry out the control variable experiment on different D_{max}, and r_1. The results are as shown in Fig. 17 and Fig. 18. The dimensions of D_{max} and r_1 are both km.

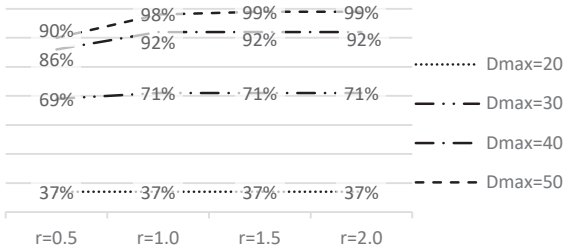

Fig. 17. The comparison of P_{min} under different r_1 and D_{max}

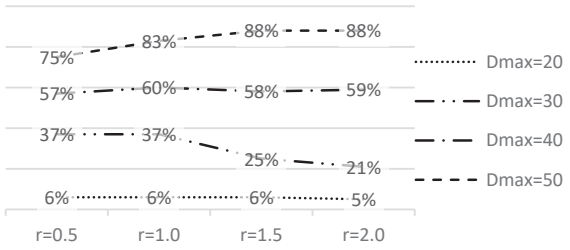

Fig. 18. The comparison of P_{min} under different r_1 and D_{max}

The simulation above proved that among the three variables in the algorithm proposed in this paper, the most influential factor is D_{max}, followed by *I*. The improvement of these two parameters can greatly improve the users' on-line rate. The impact of r_1 is not monotonically increasing or decreasing, it has a peak. A proper increase of r_1 can inhibit the turning slope of the UAV during turning, so as to ensure that the coverage of the base station is not affected. However, a large r_1 will prolong the flight cycle of the UAV, and the remote users will not be able to access the network for a long time, resulting in a reduction in the on-line rate. It is necessary to take an appropriate value for r_1.

V. CONCLUSION

This paper proposes a route planning algorithm which aims to solve the problem of setting up the maritime communication network of fixed-wing UAV communication base stations under the condition of limited resources. The route planning algorithm forms a set of route plans that can be realized by fixed-wing UAV under the constraints of the flight speed, the turning radius and turning slope, the transmission distance and the total number of the UAV communication base stations, mainly by grouping the users, setting and filtering the control points, plotting and smoothing the route patterns.

The above results have proved that the algorithm proposed in this paper can better play the coverage efficiency of UAV communication base stations under the condition of limited resources. The simulation results show that the average and minimum on-line rate of the users obtained by the algorithm in this paper are up to 27% and 54% higher than those obtained by the method of distributing the UAV communication base stations evenly, up to 16% and 33% higher than those obtained by the method based on K-means clustering in [6], and up to 7% and 27% higher than those obtained by the method based on the weighted centroid of the users in [7].

At the same time, this paper also lays some foundation for further optimization. This paper carries out simulation tests on the impact of different route planning parameters on the communication coverage, and discusses the impact of the total number of the UAV communication base stations, the transmission distance of the base stations, and the turning radius of the UAVs on the users' on-line rate.

The algorithm proposed in this paper can be better applied to solve the problem of setting up maritime communication network of fixed-wing UAV communication base stations under the condition of limited sources.

REFERENCES

[1] Cai Jian. Overview of UAV application and development in various countries. [J]. China Security, 2016, No.132(09):91-103.

[2] Samira Hayat, Evsen Yanmaz, and Raheeb Muzaffar. Survey on Unmanned Aerial Vehicle Networks for Civil Applications: A Communications Viewpoint. [J]. IEEE Communications Surveys and Tutorials, 2016, 18(4).

[3] Wang Qiming. Research on Algorithm of Air-ground Cooperative Path Planning for Man-machine Formation. [D]. Harbin Institute of Technology, 2021. DOI:10.27061/d.cnki.ghgdu.2021.003962.

[4] Xuan Mengli. Mission planning of UAV formation. [D]. Xi'an University of Electronic Technology, 2020. DOI:10.27389/d.cnki.gxadu.2020.000747.

[5] Zhu Shiren. Research on communication support in mountain and jungle area based on UAV formation. [D]. National University of Defense Technology, 2019. DOI:10.27052/d.cnki.gzjgu.2019.001005.

[6] Wang Hua. Research on coverage deployment method of UAV air base station. [D]. Xi'an University of Technology, 2020. DOI:10.27398/d.cnki.gxalu.2020.000726.

[7] Xu Zanxin, Yuan Jian, Wang Yue, Zhang Yaodong, Yi Longteng, Huo Jinhai, et al. A Multi-UAV Relay Network Supporting Mobile Ad Hoc Network Communication. [J]. Journal of Tsinghua University (Natural Science Edition), 2011, 51(2):150-155.

[8] Zhao Yanhao. Research on simulation algorithm of takeoff and go-around track of domestic civil aircraft. [D]. China Civil Aviation Flight Academy, 2017.

[9] Dai Yasheng, Ma Bailin, Le Guangxue. Fading estimation model of marine wireless communication channel in complex meteorological environment. [J]. Telecommunications Science, 2022, 38(03):158-171.

[10] Chen Liang, Jin YongXing, Hu Qinyou, Tang Kecheng, Gao Wanming. Transmission loss of marine VHF wireless communication. [J]. Chinese navigation, 2015, 38(03):1-4.

[11] MiniakGórecka Alicja,Podlaski Krzysztof,Gwizdałła Tomasz. Using K-Means Clustering in Python with Periodic Boundary Conditions[J]. Symmetry, 2022, 14(6).

[12] Classification of the Dubins set. [J]. Andrei M. Shkel, Vladimir J. Lumelsky. Robotics and Autonomous Systems. 2001 (4).